The Influence of Beam Injection Geometry upon Transport and Current Drive in the MAST Spherical Tokamak

R.J. Akers 1), L.C. Appel 1), P.G. Carolan 1), I. Chapman 1), N.J. Conway 1), G.F. Counsell 1), G. Cunningham 1), E. Delchambre 1), M.R. Dunstan 1), A.R. Field 1), S. Gee 1), P. Helander 1), D. Keeling 1), A. Kirk 1), S. Lisgo 2), B. Lloyd 1), D.G. Muir 1), A. Patel 1), R. Scannell 1), K.Stammers 1), D. Taylor 1), A.Thyagaraja 1), M.R. Tournianski 1), M. Valovič 1), M.J. Walsh 1) and the MAST and NBI teams.

1) EURATOM/UKAEA Fusion Association, Culham Science Centre, Abingdon, UK.
2) University of Toronto Institute for Aerospace Studies, Toronto, Canada.

e-mail contact of main author: rob.akers@ukaea.org.uk

Abstract

MAST (R=0.85m, a=0.65m, κ~2.2, B_ϕ~0.4T, I_p~1MA) is currently equipped with two co-tangential neutral beam injectors (each delivering up to P_{NBI}=2.5MW, E_0~40-60keV D beams), engineered for optimal core heating efficiency and resulting in peaked heating and current drive profiles. This geometry has been successful in generating high performance, high beta discharges in a range of plasma regimes (L-mode, ELMing and ELM free H-mode, ITB plasmas etc.) and has provided a suitable platform for studying Spherical Tokamak plasmas with currents I_p>1MA. In order to achieve "steady state", sawtooth-free operation at I_p~1MA (in the absence of any MHD redistribution of the current profile), 0D assumptions for confinement scaling together with TRANSP simulations indicate that a combination of off-axis, and co- and counter- directed mid-plane beams are required. Similarly, power-plant and component test facility (CTF) designs require both on and off-axis NBI. In this paper we discuss experiments which have been performed in order to study the influence the NBI geometry has upon plasma performance on MAST, exploiting strongly up-down asymmetric Single Null Diverted (SND) discharges and the ability to reverse the plasma current and toroidal field. Results from integrated transport analysis are being used to design a possible upgrade to the MAST NBI systems and load assembly and for designing future devices such an ST Component Test Facility.

1. Introduction

Next generation Spherical Tokamak (ST) designs require a large pressure driven component of plasma current, combined with efficient off-axis auxiliary current in order to guarantee, in the absence of any MHD driven redistribution of the current profile [1,2], central safety factors q_0>1 (thereby avoiding sawtooth driven seeding of neoclassical tearing modes). For example, the Culham ST power plant (STPP) design [3] requires ~15MW of 50keV off-axis neutral beam current drive (NBCD) to generate an MHD stable, steady-state plasma; similarly CTF designs require ~40MW of 150keV off-axis CD [4]. Off-axis NBCD is also used in conventional tokamaks and shows some unexpected behaviour (in particular on ASDEX Upgrade [5]). On MAST, two 2.5MW, 40-60keV beam-lines are orientated in the mid-plane, both pointing in the same direction with a tangency radius of ~0.7m (~1 fast ion Larmor radius inboard of the magnetic axis R_{mag}~0.9m). The system is optimized for efficient core heating using co-injection, and has been successful in delivering high performance plasmas [6]. However, for the densities required for efficient NBCD on MAST ($n_e(0)<3\times10^{19}/m^3$), this geometry results in large radius sawteeth and a corresponding reduction in plasma performance. To achieve long pulse discharges, it is necessary therefore, to modify the NBI injection geometry to drive current further towards the plasma periphery. TRANSP [7] simulations, assuming classical fast ion behaviour, suggest that a combination of off-axis and co- and counter-directed mid-plane beams will be suitable for sustaining fully relaxed, 5s pulses with q_0>1, thereby providing a platform for studying plasma regimes closer to those required for STPP and CTF, as well as providing a major extension to the

capabilities of MAST in support of studies for ITER. A number of experiments are being performed in order to confirm predictions for reorienting the beams. Although the existing beam-lines themselves cannot easily be moved, changes to the NBI geometry can be effected by either a) reversing I_p (producing counter- rather than co-injection) and/or b) moving the plasma vertically either to a Lower (L) or Upper (U) SND configuration (resulting in off-axis injection). In this paper we discuss these three regimes and the resulting impact upon energy confinement and current drive.

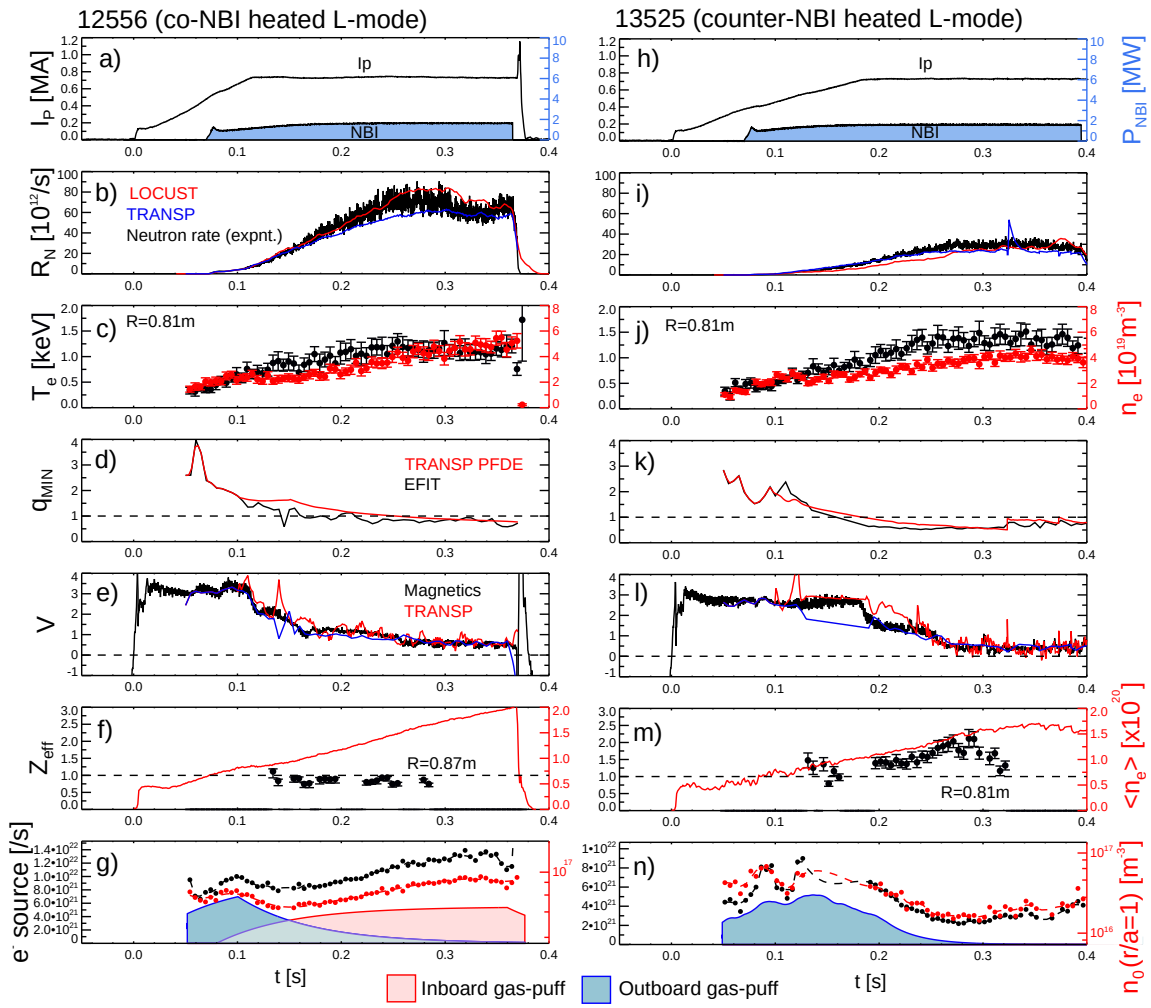

Fig.1: Experimental and model time traces for a typical co-NBI heated L-mode discharge (left) and L-mode counter-NBI heated L-mode discharge (right). a) and h) show I_p and NBI power, b,i) measured and modelled neutron rate, c,j) $T_e(0)$ and $n_e(0)$, d,k) EFIT and TRANSP $q_{min}(t)$, e,l) magnetics and TRANSP (red) loop voltage V_{loop}, f,m) core $Z_{eff}(t)$ and line integral density and g,n) e^- source (assuming uniformity around the separatrix) , edge neutral density and gas flow.

2. Co-injection heated L and H-mode discharges

Mid-plane tangential co-NBI is effective in heating the plasma and delivering the beta values required for evaluating the potential of the ST as a future fusion reactor or CTF. Both L- and H-mode co-NBI heated plasmas are routinely studied with ELMing H-mode discharges exhibiting energy confinement in line with scaling law IPB98[y,2] [8] and L-mode showing a trend with plasma current similar to that given by L97 [8] ($\tau_E \propto I_p^{0.96}$). Transport and neutral

beam heating simulations have been carried out using TRANSP and the full gyro-orbit simulator LOCUST [9]. A new charge exchange recombination spectroscopy (CXRS) system has now been fully commissioned, providing, for the first time on MAST, time evolving high resolution (~Larmor orbit scale) ion temperature and carbon rotation profile data, thereby allowing the time evolution of transport coefficients to be studied in detail. Other improvements to the analysis include the introduction of a high resolution time resolved edge Thomson Scattering system [10], confirmation of the MAST neutron detector calibration using Indium foil activation measurements and the implementation of various new 2D imaging systems (for example Beam Emission Spectroscopy (BES) and improvements to the 2D bremsstrahlung camera used for determining Z_{eff} [11].). Fig. 1a-g) shows time traces for a typical sawtooth free L-mode plasma, one of a series of similar discharges where the Neutral Particle Analyser (NPA, on loan from PPPL) and high resolution core Thomson scattering laser were scanned in space (radially) and time respectively. Plasma current was ramped to 0.8MA at 120ms then held flat until 330ms. 2MW of co-NBI was injected using a single 40keV D source from 90ms onwards, and gas puffing provided (fig.1g) using both inboard (pink) and outboard (light blue) valves, resulting in a core $n_e(0)$ of ~$4.5x10^{19}/m^3$, an edge neutral density at the low field side of ~$8x10^{16}/m^3$, $T_e(0)$ ~1.2keV and neutron rate of ~$7x10^{13}/s$. Analysis of 2D BES imaging data reveals a reduction in power below that originally assumed during the time when the NBI injector was significantly off-perveance. BES data have therefore been used to calibrate the NBI input power. TRANSP and LOCUST indicate that ~75-85% of the power was absorbed, with both models providing a good fit to the flat-top neutron rate (fig.1b). Core Z_{eff} was flat and ~1 for most of the discharge with solution of the poloidal field diffusion equation (PFDE) yielding a reasonable match to the time evolution of q_{min} when compared with magnetic equilibrium reconstruction (EFIT [12], including kinetic constraints and toroidal rotation) and a good match to the measured loop voltage (fig.1e) (bootstrap fraction ~15%, NBCD fraction ~10%). The plasma neutral density profile required by the simulations was determined using an absolutely calibrated, mid-plane high resolution linear D-alpha array combined with Thomson scattering and Langmuir probe data (which are used to augment the edge T_e and n_e profiles by deploying a 2-point edge model) and the FRANTIC [13] neutrals model used to extrapolate the profile into the plasma core. In order to match the incident flux (determined by radially integrating the D-alpha emission converted into ionization rate using ADAS [14] atomic database rate coefficients), a neutral temperature of ~5eV is required (in good agreement with KN1D [15] neutrals simulations based upon Thomson scattering and

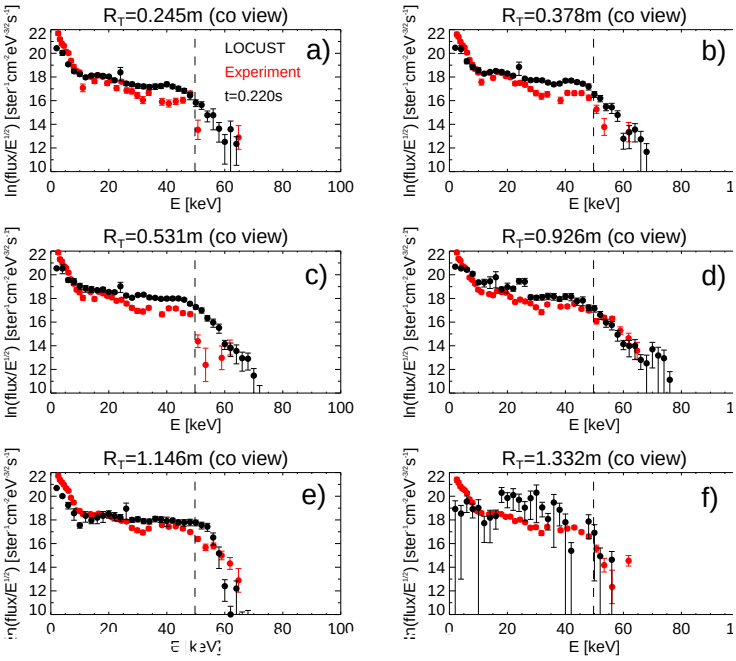

Fig. 2: Modelled (black) vs. experimental (red) NPA spectra @220ms and various NPA tangency radii for co-NBI heated L-mode discharge 12556.

fast ion gauge data). Both LOCUST and TRANSP model the fast ion distribution function by

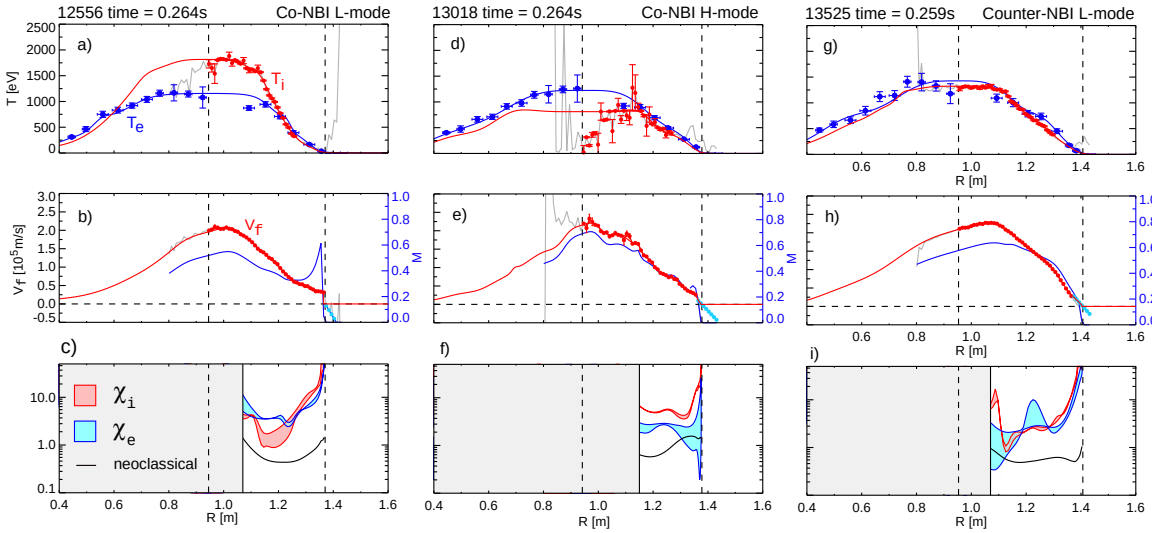

Fig.3: Kinetic profile data and energy diffusivities for co-NBI heated L-mode discharge 12556 @264ms, co-NBI heated H-mode discharge 13018 @264ms and counter-NBI heated L-mode discharge 13525 @259ms. a,d,g) show Ti and Te, b,e,f) Vϕ and Mach number relative to the thermal deuterium sound speed and c,f,i) χ_i and χ_e.

simulating electron drag, thermal ion scattering, energy diffusion and charge exchange driven cross field transport and loss. The LOCUST NPA model includes higher order effects such as finite neutral seed energy and a Monte Carlo calculation of the beam halo for the active spectrum together with finite plasma rotation for producing the doppler shifted thermal energy distribution. Fig. 2 shows NPA spectra for different tangency radii at 220ms with experimental data in red and LOCUST simulations including Monte Carlo errors in black. Preliminary simulations indicated a discrepancy above primary injection energy in the core using both LOCUST and TRANSP, with experimental spectra displaying a tail out to >60keV. A similar effect has been achieved here using LOCUST by doubling the energy diffusion operator. The discrepancy is likely due to fast ion "knock-on" self collisions (omitted in the simulations) – indeed, a similar result was reported for CLEO [16] where the measured tail was four times that predicted by Fokker Planck modelling of thermal-tail driven diffusion alone. Other possibilities include the presence of fast particle MHD, as these discharges contained a rich variety of Toroidal Alfvén Eignemode (TAE) and chirping activity. Interestingly, there is some evidence that "core" fast ions (fig. 2c) may be subject to some level of redistribution (as described for NSTX in [17]), however further work is needed to eliminate sources of systematic error (for example, the influence of a substantial molecular density outside the separatrix (n_{D2}~10^{18}/m^3), possible mis-interpretation of q(0), uncertainty in the beam species mix, time variation of the edge neutral temperature or the balance between cold and hot recycling neutral sources). Nevertheless, spectra do indicate a good level of fast ion confinement, which when combined with the match between modelling and experiment of the neutron rate and power collected at the target Langmuir probes, support the measured confinement times and level of plasma performance.

Figs 3 a-c) show the electron and ion temperature at 264ms, the plasma rotation profile resulting from the 2MW of co-tangential injection and the ion and electron diffusivities χ_i and χ_e, determined using TRANSP. At 140ms, ion and electron diffusivity were large at around

~5-10m^2/s in the core, rising to well above 10m^2/s in the pedestal region. An ion barrier then started to form in the plasma core and moved radially outwards, resulting in diffusivities of order 2-4m^2/s at 264ms (~2x neoclassical) in the half radius region of the plasma, rising to a level of 5-8m^2/s in the pedestal (R~1.3m). τ_E at this time was ~31ms, corresponding to an enhancement over IPB98[y,2] scaling of H_H~0.94, i.e. almost as high as typical H-mode discharges. Co-incident with the location of the ITB, defined here at the maximum of ρ_s/L_{Ti}~0.15, where ρ_s is the ion Larmor radius at the sound speed and L_{Ti} is the ion temperature gradient scale length, the ExB shearing rate ω_{SE} also peaked at ~6x10^5/s (similar in magnitude to analytic estimates of the linear growth rate of ITG modes). Preliminary poloidal CXRS measurements for NBI heated MAST discharges indicate that poloidal rotation is low (<10km/s), the dominant contribution to ω_{SE} therefore being from the gradient of the driven toroidal flow ω_ϕ which reached 2x10^5/s on axis, corresponding to a toroidal Mach number of ~0.65. Solution of the PFDE suggests that the ITB first formed when the q=3/2 rational surface appeared in the plasma and then moved outwards as the q-profile evolved, remaining just inside this surface.

The L-mode regime described thus far can be forced into H-mode by modifying the up-down balance of the plasma and adjusting the gas fuelling [18]. Plasma evolution in H-mode was identical to that of the sawtooth free L-mode scenario up until ~160ms when the L-H transition took place. It was not possible in this case to use kinetics data for calculating W_{MHD} during H-mode as the 40keV beam provided insufficient penetration into the plasma core (due to broadening of the density profile and the formation of "ears"), however magnetics analysis indicates an improved W_{MHD} for this discharge over L-mode of around 20% when the plasma became ELM free at 240ms (in line with previously published results [6]). Figs. 3d-f) show the kinetic profiles and transport coefficients for H-mode discharge 13018 at 264ms. The enhanced confinement is, as expected, due to a reduction in transport in the pedestal where χ_i and χ_e were reduced to ~4 and ~2m^2/s respectively. A region of increased rotational shear can also be seen at this radius (ω_{SE}~7x10^5/s @r/a~0.7). It is expected that the new, highly collimated, high intensity MAST PINI NBI sources (P_{NBI}=2.5MW, E_0>60keV) will provide adequate illumination of the plasma centre for studying core confinement in H-mode.

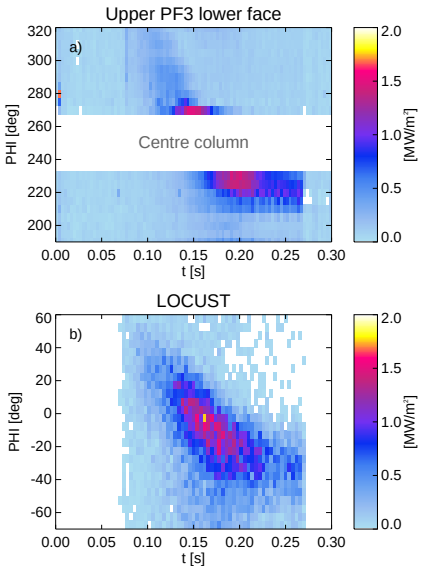

Fig.4: a) Orbit loss power loading to the upper poloidal field coil PF3 from I.R. image analysis vs. toroidal angle and time and b) the model prediction from LOCUST.

3. On-axis counter-NBI heated discharges

TRANSP simulations suggest that to generate sawtooth free, 5s MAST pulses with q_0>1, 2.5MW of counter-NBI is needed to reduce the core current driven by the mid-plane tangential co-NBI. 40-60keV counter injected deuterium orbits are, however, only weakly confined by the MAST field. Temporally evolving, poloidally and toroidally localised hot-spots can be identified throughout the MAST vessel with orbit losses of order ~50-70% being confirmed by comparing Langmuir target probe data with modelling, and analysis of the evolution of 2D infra-red images with power loading predictions from full gyro-orbit simulations. Fig. 4a) shows the evolution of power loading

for discharge 13530 to the lower face of one of the upper, in vessel poloidal field coils (PF3) (the region which received the largest flux due to fast ion orbits on their outer co-leg) against toroidal angle and time assuming "316 stainless steel" thermal properties and half the emissivity of graphite. The blanked out strip is due to the heated region being occluded by the centre column. The motion of the toroidal location of the peak flux is due to the evolving poloidal field; when the NBI terminated at 270ms, the flux rapidly disappeared (in less than 3ms, the frame capture time of the camera), compared with ~18ms for the neutron flux, confirming that heat flux was due to the prompt loss of poorly confined orbits. Fig. 4b) shows the LOCUST prediction for this discharge (whereby orbits were followed for three mid-plane transits of the instantaneous guiding centre), demonstrating an excellent level of agreement (corresponding to a peak power loading of 1.5MW/m^2), providing strong support for the modelled first orbit losses.

Even though only a fraction of the injected power was absorbed by the plasma, counter-NBI resulted in a hot plasma with temperatures rivalling those of co-NBI (which is interestingly qualitatively predicted by 2-fluid MHD turbulence simulations), corresponding to an increase in confinement time by a factor ~1.5-2 over L-mode. Fig.1 h-n) shows time traces for discharge 13525, part of a scan similar to that described for the L-mode regime. The NBCD available with <2MW of NBI is insufficient (non inductive CD fraction f_{NI}~14%) to stymie the onset of the q=1 surface, with in this case, the first sawtooth appearing at ~320ms. Indeed, sawtooth period is clearly correlated with plasma rotation speed and direction, with a minimum value for finite counter-NBI power when the driven rotation balances the intrinsic ion diamagnetic flow (with experimental data in good agreement with MISHKA-F simulations [19]). Neutron rate in the flat top is well modelled by both LOCUST and TRANSP, and is approximately half that for the co-NBI L-mode series of discharges. Z_{eff} was well controlled at a level below 2, and TRANSP simulations of the temporal evolution of q_{min} and V_{loop} agree well with experiment. For counter-NBI, the torque driven shearing reinforces the natural rotation of the plasma, and the large losses produce an enhanced torque via the JxB force of the resulting radial ion current. Density profiles are skewed towards the low field side (consistent with rotation levels which can approach Mach ~1 [20]), the resulting radial electric field combining with the JxB loss current to provide pedestal ohmic heating of order ~0.1 P_{NBI} [21]. In addition, n_e profiles are more peaked compared with co-NBI due to the increased Ware pinch (partly due to the larger Z_{eff}~2) and an inwards directed NBCD driven particle pinch [22]. This results in a reduction in the amount of gas puffing required to sustain a given line average density (comparing for example fig.1g) with fig.1n), a corresponding decrease in the edge neutral density (by a factor ~ 5) and a decrease to the thermal charge exchange drag in the plasma periphery (which is significant on MAST for co-NBI and dominates over the injected torque profile in the outer third of the plasma). Plasma toroidal rotation is, as a result, much broader (fig 3h), providing much greater ExB shear at the edge, the likely cause of the reduced peripheral transport and broader T_e profiles observed during counter-NBI [20]. Fig. 3i) shows the transport coefficients at 259ms, revealing that χ_i and χ_e are reduced to 2-3m^2/s across

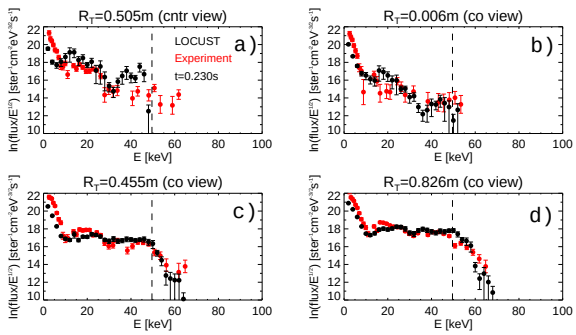

Fig.5: Experimental and modelled NPA spectra for various co and counter pointing NPA chords in counter-NBI heated discharge 13525.

most of the plasma, below levels observed for co-NBI heated L and H-mode plasmas. Work is underway to design a cryo-pumped, closed divertor in order to deliver greater density control and reduce separatrix neutral density, in the hope that edge rotational shear can be increased in co-NBI heated discharges, resulting in plasma performance closer to that observed during counter-NBI.

4. Off-axis NBI

STPP, CTF and MAST will all likely require off-axis NBCD in order to prevent the appearance of the q=1 surface whilst at the same time driving an appreciable fraction of the plasma current. Due to the large B_{pol}/B_{tor} ratio in the ST, the resulting NBCD profile for horizontally oriented off-axis NBI is predicted to be significantly different if the beam is injected above, rather than below the magnetic axis, thereby providing a means of testing NBI model predictions of the driven current for low NBCD fraction. Experiments have been performed in LSND and USND discharges with I_p~0.7MA, $\langle n_e \rangle$~$2x10^{19}/m^3$, $T_e(0)$~1keV and NBCD fraction ~25%, with plasma stored energy and neutron rate well modelled by TRANSP. Fig. 6 shows various data for the SND discharges together with ohmic reference plasmas, vs. vertical offset of the beams w.r.t. Z_{mag}. Discharges exhibited electron temperatures (with T_e for lower and upper diverted discharges carefully matched), confinement, neutron rates etc. comparable to on-axis co-NBI heated plasmas. As predicted, sawtooth onset time was delayed by typically ~70ms and l_i was lower for LSND. TRANSP modelling of a typical U-SND/L-SND pair (16391 & 16392) indicates a similar delay to the q=1 onset time of ~65ms, although the systematic error when solving the PFDE due to the initial choice of q-profile is typically large. It is also notable, however, that the modelled loop voltage across a wide range of discharges is consistent with that expected from theory. Fig. 7 shows TRANSP versus measured loop voltage for discharges studied so far with the newly available diagnostic set (including all discharges in this paper). There is a small discrepancy, partly due to motion of the inner separatrix close to the measurement coils. Taking this into account produces a better 1:1 correlation but with significantly increased scatter. In addition, there are many systematic errors in the large quantity of data deployed in the modelling which could contribute a discrepancy of around 5-10%. f_{NI} for the discharges shown varies between 0 and 35%, however there is no clear correlation of f_{NI} with loop voltage discrepancy (correlation coefficient= 0.20), suggesting that the sum of the pressure driven current fraction and NBCD on MAST is in good agreement with theory.

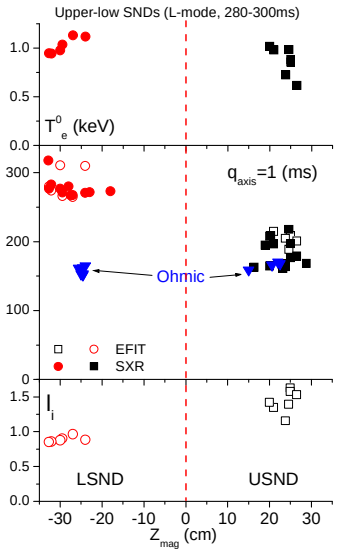

Fig.6: $T_e(0)$, sawtooth onset time and li vs. NBI Z-offset.

5. Discussion

TRANSP NBI simulations, assuming established fast ion coulomb collision theory and IPB98[y,2] confinement scaling, indicate that to achieve 5s, sawtooth free, I_p~1MA operation of the MAST device, >5MW of NBI will be required, made up of a combination of core co- and counter directed as well as off-axis sources. Transport simulations which exploit recent advancements to the MAST diagnostic set, are allowing studies of the influence of NBI

injector geometry upon plasma performance. Co-heated L-mode discharges routinely show evidence of an outwardly evolving core ITB, with confinement approaching that of H-mode. Confinement in H-mode exceeds that of L-mode due to a reduction in transport in the plasma periphery, with confinement scaling in line with IPB98[y,2] scaling. Counter-NBI discharges show a factor of ~2 enhancement in confinement over typical co-NBI heated plasmas, resulting in similar levels of plasma performance (even with only ~50% of the NBI power absorbed). The improvement in confinement appears to be due to a reduction in transport as a result of increased peripheral ExB shearing. Simulations of the NPA spectrum for co- and counter-NBI heating, and direct measurements of the prompt fast ion loss during counter-NBI using infra-red imaging, support the assumption that fast ion behaviour is well described by established NBI theory. Strongly up-down asymmetric SND discharges, with similar confinement to double null diverted plasmas, are also well modelled by TRANSP, with q=1 onset delayed by ~60ms (for P_{NBI}~2MW) in LSND compared with USND, as expected, and measured loop voltage in good agreement with that predicted by solving the current diffusion equations. Increases to the amount of available NBI power and commissioning of a new MSE system will allow more detailed studies over the coming year, and in particular should help to uncover any anomalous behaviour of the fast ions, providing further input to the design of ST based CTF designs and a possible future upgrade of the MAST NBI systems.

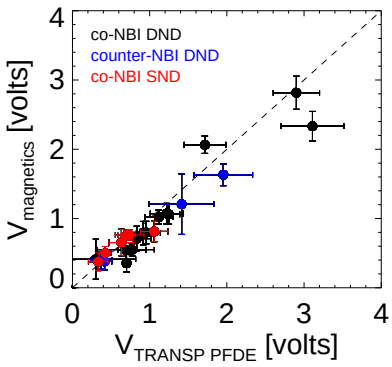

Fig. 7: Measured vs. modelled V_{loop}.

References

[1] A.Sipps, J.Hobirk & A.G.Peeters, Fusion Science & Technol. 44 605.
[2] T.Luce et al., Nucl. Fusion. 43 321 (2003).
[3] R.J.Akers et al., Nucl. Fusion, Vol. **40**, No. 6 (2000) 1223.
[4] A.W.Morris et al., Fusion Engineering & Design, 74 67 (2005).
[5] S.Günter et al., 20th IAEA Fusion Energy Conference, Vilamoura, Portugal, 2004 (IAEA-CN-116/OV/1-5).
[6] R.J.Akers et al., Physics of Plasmas, 9 9 3919 (2002).
[7] R.J.Hawryluk 1980 An empirical approach to tokamak transport Physics of Plasmas close to Thermonuclear Conditions vol 1, ed B.Coppi et al. (Brussels: CEC) p19.
[8] ITER Physics Basis, Nuclear Fusion 39 12 2175 (1999).
[9] R.J.Akers et al., Nucl. Fusion 42 122 (2002).
[10] R.Scannel et al., submitted to Rev. Sci. Inst.
[11] A.Patel et al., Rev. Sci. Inst. 75 11 4944 (2004)
[12] L.L.Lao et al., Nucl. Fusion 25 1611 (1985).
[13] S. Tamor, J. Comput. Phys. 40 104 (1981).
[14] For a full description of the code see: http://www.adas.co.uk/
[15] B.LaBombard, Plasma Science and Fusion Center Research Report PSFC-RR-01-3 (2001).
[16] J.G.Cordey & W.G.F.Core, Phys. Fluids 17 1626 (1974).
[17] J.E.Menard et al., "Observation of Instability-induced Current Redistribution in a Spherical Torus Plasma", submitted to PRL.
[18] H.Meyer et al., Plasma Physics Control. Fusion 47 1 (2005).
[19] S.Pinches et al., this conference, paper EX/7-2Ra.
[20] R.J.Akers et al., 20th IAEA Fusion Energy Conference, Vilamoura, Portugal, 2004 (EX/4-4).
[21] P. Helander, R.J. Akers, and L.-G. Eriksson, Phys. Plasmas **12**, 112503 (2005).
[22] P. Helander and R.J. Akers, Phys. Plasmas **12**, 042503 (2005)

Acknowledgements. This work was jointly funded by the UK Engineering and Physical Sciences Research Council and by the European Communities under the Contract of Association between Euratom and UKAEA. The views and opinions expressed herein do not necessarily reflect those of the European commission. NBI equipment is on loan from ORNL and the NPA from PPPL.